MIXING IN SWIRLING JET

CHIAKI KURODA, KOHEI OGAWA AND ICHIRO INOUE
Department of Chemical Engineering, Tokyo Institute of Technology, Tokyo 152

Key Words: Mixing, Swirling Jet, Swirl Reynolds Number, Reynolds Number, Variance Coefficient, Peclet Number

The relationship between the mixing process in a swirling jet and operational parameters Re and Re_θ, which are respectively the general Reynolds number based on cross-sectional average velocity in a jet nozzle and the newly defined swirl Reynolds number based on characteristic angular velocity of swirling motion at a nozzle exit, was investigated by measuring concentration distributions of expanding tracer puffs.

It is clarified that the increase of Re promotes both radial and axial mixing, and that the increase of Re_θ greatly promotes radial mixing but suppresses the axial mixing. Considering the effects of Re_θ on the Peclet number, it is made clear that the mixing process is remarkably changed by the generation of reverse flow in a swirling jet.

Introduction

The flow behavior of a swirling jet is much different from that of a non-swirling jet in many respects, e.g. the jet angle expanding in the radial direction, the axial velocity distribution, and the turbulence structure. Thus the mixing process in a swirling jet is clearly influenced by the swirling motion, and the characteristic effect is applicable to many kinds of equipment using jet mixing, such as spray dryers and combustion furnaces. A swirl burner is a typical example, and many investigations[3,5,7,8] have been made with respect to the thermodynamic and aerodynamic structure of swirling flames. In such reacting flows, the mixing process of chemical species is a very important factor in the performance of the equipment. There have been, however, only a few previous reports[1,2,6] about swirling jet mixing, and the mixing process within a swirling jet and its dependency on the operational conditions have not yet been sufficiently clarified. One reason is that there have been few detailed investigations of the factors which influence flow behavior.

The present work investigates the factors that influence flow behavior, which controls most of the mixing process in a swirling jet and examines experimentally the mixing process within a swirling jet of water, as compared with a non-swirling jet, by measuring concentration distributions of a liquid tracer. It makes clear the effects of the operational conditions, especially the intensity of swirl, on the mixing process.

Received December 8, 1984. Correspondence concerning this article should be addressed to C. Kuroda. I. Inoue is now with Dept. of Chem. Eng., Kogakuin Univ., Tokyo 160.

1. Important Dimensionless Factors for a Swirling Jet Flow

It is considered suitable to study vortex motion such as a swirling jet flow by the following vorticity equation:

$$\frac{\partial \boldsymbol{\Omega}}{\partial t}+(\boldsymbol{U}\cdot\nabla)\boldsymbol{\Omega}-(\boldsymbol{\Omega}\cdot\nabla)\boldsymbol{U}=\nu\nabla^2\boldsymbol{\Omega} \tag{1}$$

In this paper, some dimensionless factors that are important in expressing the operational conditions of swirling jet equipment are derived from Eq. (1). In swirling flow, as was made clear in the previous paper,[4] the vortex motion around the center axis influences the flow behavior, and the characteristic angular velocity ω_i of the vortex motion should be treated as a key velocity. In a normal jet flow, the cross-sectional average velocity U_a in the jet nozzle is usually used as a characteristic velocity. Therefore, it is reasonable to use the above characteristic velocities ω_i and U_a, which are measured at the exit of the jet nozzle, to provide the dimensionless quantities of the vorticity $\boldsymbol{\Omega}$ and the velocity $\boldsymbol{U}$ in the vorticity equation. As a result, the following three types of dimensionless equations are derived according to the arrangement of the dimensionless terms:

$$\frac{\partial \boldsymbol{\Omega}^*}{\partial t^*}+\frac{U_a}{R\omega_i}\{(\boldsymbol{U}^*\cdot\nabla^*)\boldsymbol{\Omega}^*-(\boldsymbol{\Omega}^*\cdot\nabla^*)\boldsymbol{U}^*\}=\frac{\nu}{R^2\omega_i}\nabla^{*2}\boldsymbol{\Omega}^* \tag{2a}$$

$$\frac{R\omega_i}{U_a}\frac{\partial \boldsymbol{\Omega}^*}{\partial t^*}+(\boldsymbol{U}^*\cdot\nabla^*)\boldsymbol{\Omega}^*-(\boldsymbol{\Omega}^*\cdot\nabla^*)\boldsymbol{U}^*=\frac{\nu}{RU_a}\nabla^{*2}\boldsymbol{\Omega}^* \tag{2b}$$

$$\frac{R^2\omega_i}{\nu}\frac{\partial \boldsymbol{\Omega}^*}{\partial t^*}+\frac{RU_a}{\nu}\{(\boldsymbol{U}^*\cdot\nabla^*)\boldsymbol{\Omega}^*-(\boldsymbol{\Omega}^*\cdot\nabla^*)\boldsymbol{U}^*\}=\nabla^{*2}\boldsymbol{\Omega}^* \tag{2c}$$

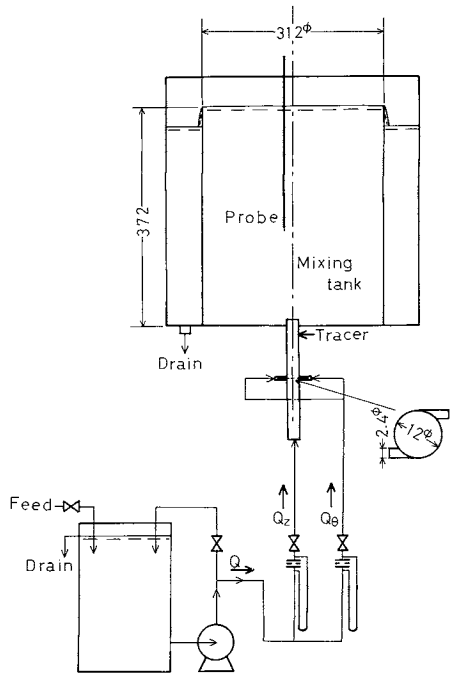

Fig. 1. Experimental apparatus.

where * denotes a dimensionless quantity. The characteristic length and time are the inner radius R of the jet nozzle and ω_i^{-1}, respectively.

In the above three types of dimensionless equations, there are three common dimensionless quantities, namely the general Reynolds number $2RU_a/\nu$, a kind of Reynolds number $R(R\omega_i)/\nu$ based on the characteristic angular velocity and the ratio of rotating velocity to axial velocity $R\omega_i/U_a$. These quantities are considered to be important as dimensionless factors in expressing the operational conditions of a swirling jet and to be related with the flow behavior and further the mixing state. Only two dimensionless quantities, however, are considered to be independent factors by estimating from the number of operational variables. Actually, any one among the above three dimensionless quantities can be expressed as a quotient of the other two quantities. In this study, two kinds of Reynolds numbers, namely the general Reynolds number Re $(=2RU_a/\nu)$ and the Reynolds number of swirl Re_θ $(=R(R\omega_i)/\nu)$ will be used.

2. Experimental

Figure 1 shows a schematic diagram of the experimental apparatus, which consists of an acrylic-resin jet mixing tank with an inside diameter of 312 mm and a height of 372 mm. A jet nozzle with an inside diameter of 12 mm is set at the center of the tank bottom.

The test fluid, water, is supplied into the nozzle pipe through two entrances. One is an axial entrance from which the test fluid is supplied with the flow rate Q_z, and the other is a tangential entrance from which the test fluid is supplied with the flow rate Q_θ. The total flow rate Q is the sum of Q_z and Q_θ.

Table 1. Operational conditions

Re [—]	Re_θ [—]	Key	Re [—]	Re_θ [—]	Key
5100	2300	◑	6800	0	△
6800	2300	○	6800	1500	□
8300	2300	◐	6800	2300	○
10500	2300	◓	6800	3600	▽
			6800	5700	◇

The circular tank used is surrounded by a water-filled rectangular tank, and some visualization experiments were performed by using dyes and polystyrene particles.

The operational conditions, namely the above two Reynolds numbers Re and Re_θ, are changed by adjusting Q and Q_θ. The characteristic velocities U_a of Re and $R\omega_i$ of Re_θ are obtained by $U_a=Q/\pi R^2$ and $\omega_i=\Gamma_i/2\pi R^2$ respectively (where Γ_i is the intensity of swirl (the circulation)[4] at the jet nozzle exit and can be measured practically). In this study, two experimental series of $Re=$variable, $Re_\theta=2300$ and $Re=6800$, $Re_\theta=$variable were carried out as shown in **Table 1**.

The tracer liquid used was an aqueous solution of KCl, injected into the jet nozzle just before the exit in the impulsive state using a solenoid-operated valve. The opening time interval of the valve was chosen as 0.06 s so as to become short enough compared with the time interval between the beginning and the end of the measured concentration signal in the jet region. Measurement of the tracer concentration was continuously carried out by detecting the electric conductivity of the solution. The probe used consisted of a couple of platinum wires with a diameter of 1.0 mm, a length of 8.0 mm and an interval of 2.0 mm.

The measurements were carried out at an axial interval of 20.0 mm between the nozzle exit ($z=0$ m) and $z=0.18$ m, and at a radial interval of 10.0 mm between the center axis ($r=0$ m) and $r=0.12$ m at maximum. Ten detecting trials were performed under the same operational conditions for each measuring position in order to obtain a smooth curve of concentration change.

3. Experimental Results

3.1 Visual experiments

Figure 2 shows photographs of dyed swirling jets where dyes are injected in the step state. From these results, remarkable characteristics are seen with respect to the radial expanse of the dyed region. Namely, in the case of $Re=$constant, the expanding angle in the radial direction becomes larger with increasing Re_θ, and in the case of $Re_\theta=$constant, it is

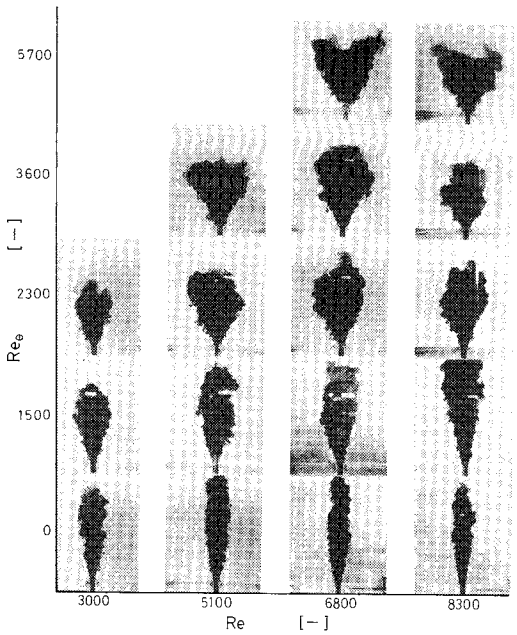

Fig. 2. Dyed region of swirling jet and operational conditions.

almost independent of *Re*. Such results seem to be consistent with the following results of tracer experiments.

The shape of the dyed region can be regarded as almost axisymmetric in any operational condition, and therefore the assumption of axisymmetry may be applied in this study.

According to the observation of flow by using polystyrene particles, the existence of reverse flow, which is characteristic in the swirling flow of large Re_θ, was confirmed near the jet nozzle in the range of about $Re_\theta > 3000$ within the present experimental conditions. This reverse flow changes the flow condition greatly and is thought to influence the mixing process in all directions.

3.2 Motion of tracer puffs

Some examples of spatial concentration distributions of tracer puffs at a certain time are shown in **Fig. 3**, which shows iso-concentration lines in an r–z plane. These figures were obtained by using the graphic program GPSL of HITACHI based on the measured discontinuous data. The numerical values shown in the figures indicate the standardized concentration by that of the original tracer liquid.

From the above figure, it can be estimated that the swirling motion promotes radial mixing, but it suppresses axial mixing and the axial travelling velocity of the tracer puffs. It is possible to predict that both mixing in all directions and axial travelling velocity are promoted by the increase of *Re*. These spatial concentration distributions are much different from those in uniform flow, owing to the complicated three-dimensional flow condition in the swirling jet. In this study, the above qualitative views are quantitatively investigated by using the mixing diffusivity (the variance coefficient) and the Peclet number, which represent the intensity of mixing and the degree of relative expanse of tracer, respectively.

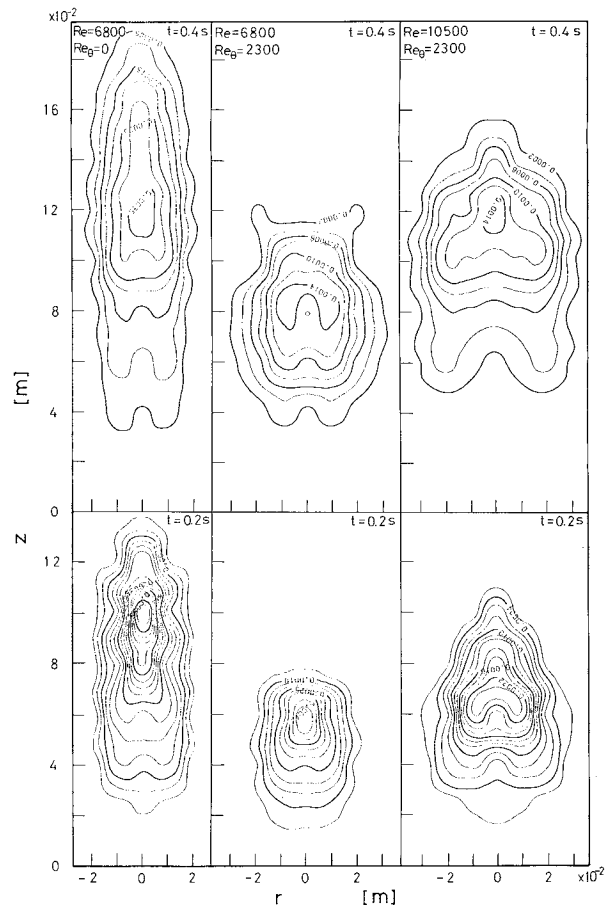

Fig. 3. Concentration distributions of tracer puffs.

4. Discussion

Based on the experimental data of impulse response tests, the mixing process in the swirling jet is investigated in relation to the operational conditions.

4.1 Average position

Assuming that the mixing state is axisymmetric, the average position (r_a, z_a) of tracer puffs is calculated at each time by using the concentration C_{ij} at every measured position (r_{ij}, z_{ij}) as follows:

$$r_a = 0 \qquad z_a = \sum_i \sum_j z_{ij} P_{ij} \tag{3}$$

$$P_{ij} = C_{ij} V_{ij} \Big/ \sum_i \sum_j C_{ij} V_{ij} \tag{4}$$

where P_{ij} is the existence probability of tracer in the region (i, j) of volume V_{ij} as shown in **Fig. 4**. It is assumed that the concentration within region (i, j) can be uniformly represented by C_{ij}.

The axial motion of tracer puffs is studied with the average position z_a of Eq. (3) as shown in **Fig. 5**. The axial travelling velocity of tracer puffs decreases with

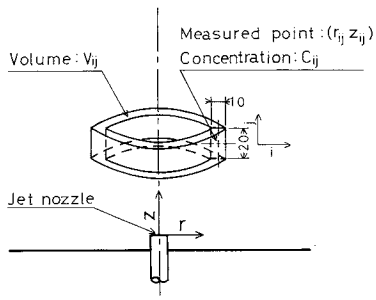

Fig. 4. Division of measuring region.

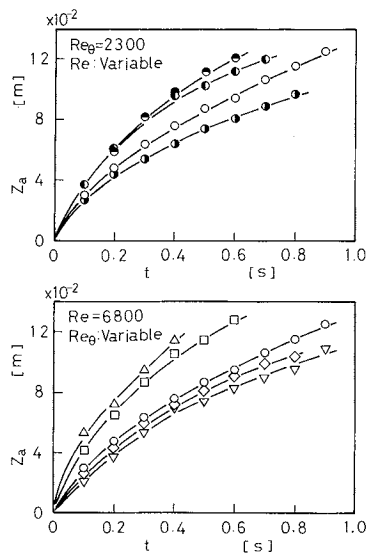

Fig. 5. Average position of tracer puffs.

increasing of Re_θ, and this result is considered to be closely connected with the axial flow velocity distributions in the swirling jet, such as the distribution with decreasing of axial velocity in the central region of the jet. In this way, Re_θ has the opposite effect on the axial travelling velocity of tracer puffs to that of Re.

4.2 Spatial variances and variance coefficients

The spatial variances of tracer expanse around the average position (r_a, z_a) are calculated at each time in order to investigate the mixing degree. Three kinds of variances, namely radial, axial and total variances, are calculated as follows:

$$\sigma_r^2 = \sum_i \sum_j (r_{ij} - r_a)^2 P_{ij} \tag{5}$$

$$\sigma_z^2 = \sum_i \sum_j (z_{ij} - z_a)^2 P_{ij} \tag{6}$$

$$\sigma^2 = \sum_i \sum_j \{(r_{ij} - r_a)^2 + (z_{ij} - z_a)^2\} P_{ij} = \sigma_r^2 + \sigma_z^2 \tag{7}$$

By using these variances, the following variance coefficients are defined in the same way as the general mixing diffusivity or the turbulent diffusivity:

$$E_r \equiv d\sigma_r^2/2dt \tag{8}$$

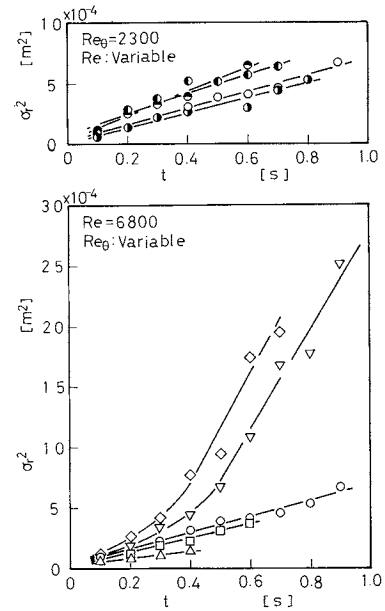

Fig. 6. Relationships between radial variance and time.

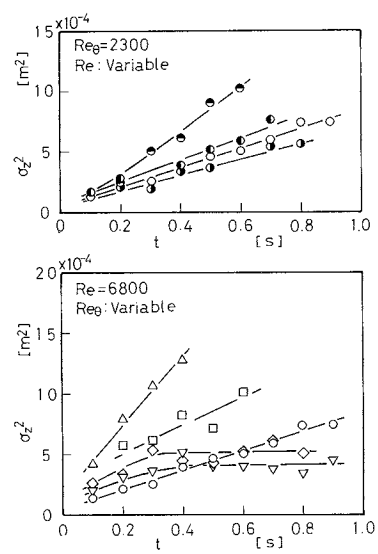

Fig. 7. Relationships between axial variance and time.

$$E_z \equiv d\sigma_z^2/2dt \tag{9}$$

$$E \equiv d\sigma^2/2dt = E_r + E_z \tag{10}$$

Considering that the average velocity field in swirling jet flow is three-dimensional and not uniform, the above coefficients include the effect of bulk diffusion as well as turbulent diffusion. In this study, however, the above variance coefficients are presumed as appropriate indexes to indicate the degree of mixing diffusion in the jet region.

The changes of variances σ_r^2, σ_z^2 and σ^2 of Eqs. (5), (6) and (7) with time are shown in **Figs. 6, 7 and 8**. The increase of Re promotes radial, axial and total mixing. On the other hand, the increase of Re_θ promotes radial mixing but suppresses axial mixing.

As seen from in Figs. 6, 7 and 8, there are linear relationships between time and the variances except

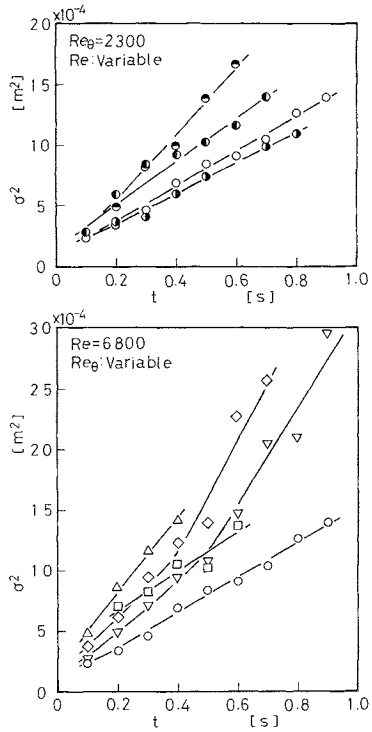

Fig. 8. Relationships between total variance and time.

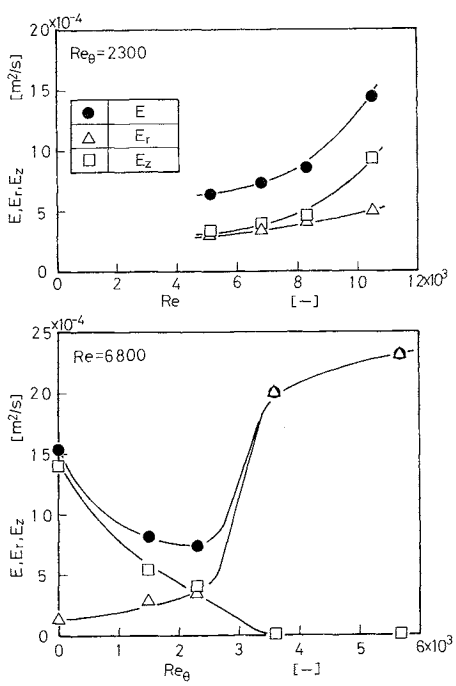

Fig. 9. Relationships between variance coefficients E_r, E_z, E and operational conditions.

for results in the initial mixing stage. From these relations, the variance coefficients E_r, E_z and E of Eqs. (8), (9) and (10) can be determined as values peculiar to each operational condition. **Figure 9** shows the relationships between E_r, E_z, E and operational conditions. The axial mixing diffusivity E_z is negligibly small in the flow conditions with reverse flow. The decrease of E_z with increasing Re_θ is considered to be

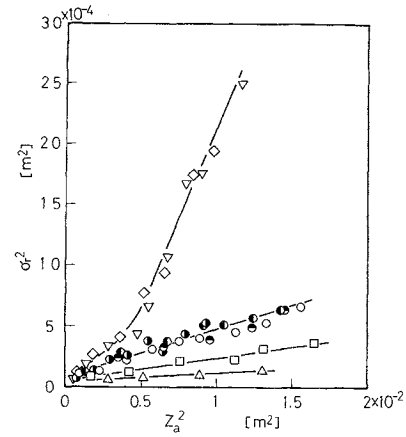

Fig. 10. Relationships between radial variance and average position.

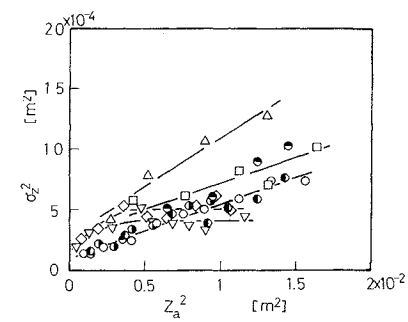

Fig. 11. Relationships between axial variance and average position.

closely connected with the decrease of the axial velocity in the central region of the swirling jet.

4.3 Peclet numbers

The Peclet number is defined by using the moved distance z_a and the travelling velocity U_m of tracer puffs as follows:

$$Pe_r \equiv U_m z_a / E_r \tag{11}$$

where the following relation is considered to be possible for U_m:

$$U_m = dz_a/dt \tag{12}$$

Consequently, from Eqs. (8), (11) and (12),

$$Pe_r = \left(\frac{dz_a}{dt} z_a\right) \Big/ \left(\frac{1}{2}\frac{d\sigma_r^2}{dt}\right)$$
$$= dz_a^2/d\sigma_r^2 \tag{13}$$

The axial and total Peclet numbers are also calculated in the same manner:

$$Pe_z \equiv U_m z_a / E_z = dz_a^2/d\sigma_z^2 \tag{14}$$

$$Pe \equiv U_m z_a / E = dz_a^2/d\sigma^2 \tag{15}$$

These Peclet numbers are considered to be dimensionless quantities which indicate the degree of relative expanse between the average distance moved by tracer puffs and the mixed distance.

To obtain the values of the Peclet numbers Pe_r, Pe_z

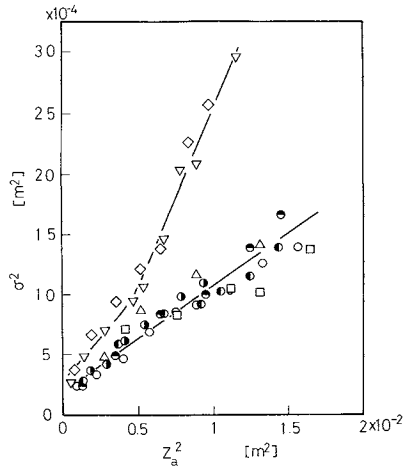

Fig. 12. Relationships between total variance and average position.

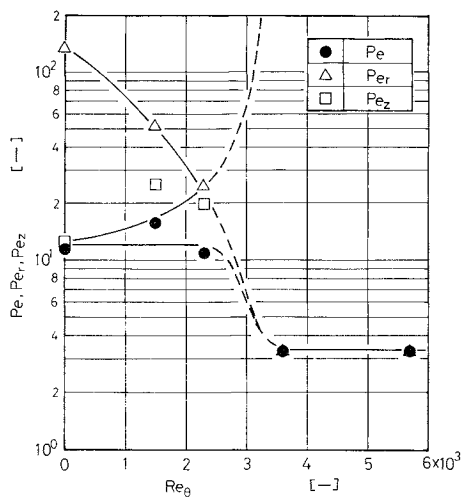

Fig. 13. Relationships between Peclet numbers Pe_r, Pe_z, Pe and Reynolds number of swirl Re_θ.

and Pe of Eqs. (13), (14) and (15), the relationships of σ_r^2, σ_z^2 and σ^2 respectively to z_a^2 are shown in **Figs. 10, 11** and **12**. There are linear relations between them except in the range of small z_a, and the Peclet numbers can be determined as values peculiar to each operational condition. Here, the effect of Re on the Peclet numbers seems to be almost negligible within the operational condition of this study, and therefore the respective relationships of Pe_r, Pe_z and Pe to Re_θ can be obtained as shown in **Fig. 13**. The result, that Pe_r is independent of Re, does not contradict the previous result by visual experiments.

As seen from the change of Pe in Fig. 13, there is a remarkable change of the mixing process near about $Re_\theta = 3000$, where reverse flow is generated. And it is seen that radial mixing mainly controls the whole mixing process in the swirling jet with reverse flow.

In this study, tracer experiments of changing Re were carried out only in the flow condition without reverse flow, and therefore it is not certain whether Re influences the Peclet numbers in the flow condition with reverse flow. From the results, however, of preliminary visual experiments, it is estimated that there is little effect of Re on the Peclet number on the whole.

Conclusions

The mixing process in a swirling liquid jet was experimentally investigated by using the impulsive tracer technique. The conclusions which could be drawn are summarized as follows:

(1) It is shown that two dimensionless quantities, the general Reynolds number Re and the Reynolds number of swirl Re_θ based on the characteristic angular velocity, validly express the operational condition of the swirling jet.

(2) An increase of Re causes the increase of radial, axial and total mixing diffusivities, while an increase of Re_θ causes the increase of radial mixing diffusivity but the decrease of axial mixing diffusivity. Total mixing diffusivity changes so as to have a minimal value with the change of Re_θ.

(3) The Peclet numbers which are defined by Eqs. (11), (14) and (15) are dependent only on Re_θ within the operational conditions of this study. A remarkable change of the mixing process is recognized near the value of Re_θ at which reverse flow is generated.

Acknowledgment

The authors wish to thank Mr. S. Niwano and Mr. T. Minato for their help in carrying out the experiments and their useful suggestions.

Nomenclature

C	=	concentration of tracer	[kg/m³]
E	=	variance coefficient	[m²/s]
P	=	existence probability of tracer	[—]
Pe	=	Peclet number	[—]
Q	=	flow rate	[m³/s]
R	=	inner radius of nozzle pipe	[m]
Re	=	Reynolds number, $2RU_a/\nu$	[—]
Re_θ	=	Reynolds number of swirl, $R(R\omega_i)/\nu$	[—]
r	=	cylindrical polar coordinate in radial direction	[m]
r_a	=	average radial position of tracer puffs	[m]
t	=	time	[s]
$\boldsymbol{U}$	=	velocity vector	[m/s]
U_a	=	cross-sectional average velocity in jet nozzle	[m/s]
U_m	=	travelling velocity of tracer puffs	[m/s]
V	=	volume of region (ij) in Fig. 2	[m³]
z	=	cylindrical polar coordinate in axial direction	[m]
z_a	=	average axial position of tracer puffs	[m]
Γ_i	=	intensity of swirl (circulation) at nozzle exit	[m²/s]
ν	=	kinematic viscosity	[m²/s]
σ^2	=	variance	[m²]
$\boldsymbol{\Omega}$	=	vorticity vector	[1/s]
ω_i	=	characteristic angular velocity, $\Gamma_i/2\pi R^2$	[1/s]

〈Subscripts〉

i, j = region (ij) in Fig. 4
r = radial direction
z = axial direction
θ = tangential direction

Literature Cited

1) Beer, J. M. and N. A. Chigier: *J. Inst. Fuel*, **42**, 443 (1969).
2) Claypole, T. C. and N. Syred: *J. Inst. Energy*, **55**, 14 (1982).
3) Gupta, A. K., D. G. Lilley and N. Syred: "Swirl Flows," Abacus Press (1984).
4) Ito, S., K. Ogawa and C. Kuroda: *Kagaku Kogaku Ronbunshu*, **4**, 247 (1978).
5) Mathur, M. L. and N. R. L. MacCallum: *J. Inst. Fuel*, **40**, 214 (1967).
6) Mathur, M. L. and N. R. L. MacCallum: *J. Inst. Fuel*, **40**, 238 (1967).
7) Sadakata, M.: *Kagaku Souchi*, **17**, 38 (1975).
8) Syred, N. and J. M. Beer: *Combustion and Flame*, **23**, 143 (1974).

(Presented at the 18th Autumn Meeting of The Society of Chemical Engineers, Japan at Fukuoka, October 1984.)

EXTRACTION KINETICS OF NICKEL WITH A HYDROXYOXIME EXTRACTANT

KATSUTOSHI INOUE, SHINICHI TOMITA AND TAKESHI MARUUCHI

Department of Industrial Chemistry, Saga University, Saga 840

Key Words: Extraction, Nickel, Hydroxyoxime, Kinetics, Complex Formation, Interfacial Reaction Mechanism

In the solvent extraction of nickel from aqueous ammonium nitrate solution with anti-2-hydroxy-5-nonylacetophenone oxime in MSB 210, measurements of initial extraction rate using a stirred transfer cell were carried out at 30°C. The extraction rate was found to be described by the rate expression

$$N=\frac{1.1\times10^{-10}[Ni^{2+}][\overline{HR}]/[H^+]}{1+1.1\times10^{-6}[Ni^{2+}]/[H^+]}$$

which was derived on the assumption that the elementary reaction step between the intermediate complex adsorbed at the interface and free extractant molecule in the aqueous phase is rate-determining. The reason why this step is rate-determining was inferred.

Introduction

Since the pioneering work by Flett *et al.*[4] on the extraction kinetics of copper with LIX 65N, an aromatic β-hydroxyoxime developed for copper hydrometallurgy, the extraction rate mechanism of copper with hydroxyoximes has been a subject attracting the interest of many researchers in the filed of solvent extraction chemistry in the last several years. Komasawa *et al.*[8] and Cox *et al.*[2] proposed the same rate expression, which is of first order with respect to metal ion and monomeric species of the extracting reagent and is of inverse first order with respect to hydrogen ion for the forward extraction rate of copper with anti-2-hydroxy-5-nonylbenzophnone oxime (the active species of LIX 65N) and anti-2-hydroxy-5-octylacetophenone oxime, respectively. Their rate expressions are based on the interfacial reaction scheme where the elementary reaction step between the intermediate complex, CuR^+, and the monomeric species of the hydroxyoxime at the interface is rate-determining.

However, this reaction scheme is against that based on Eigen's mechanism of complex formation[3] in aqueous phase, in which the ligand substitution of the reagent molecule or anion for water molecules hydrated to metal cation to form the intermediate complex is rate-determing. It can indeed give satisfactorily reasonable explanations for the rate mechanism of complex formation in the aqueous phase and that of solvent extraction of metals with the extraction reagents commonly used in analytical chemistry, which have rather high aqueous solubility and low interfacial activity. On the contrary, it cannot interprete the rate law observed in solvent extractions with commercial extracting reagents with high interfacial activity and very low aqueous solubility. Hence, it is a problem to be elucidated why the

Received December 24, 1984. Correspondence concerning this article should be addressed to K. Inoue. S. Tomita is now with Hitachi Zosen Corp., Osaka 554.